J. Cell. Mol. Med. Vol 13, No 8B, 2009 pp. 2724-2735

# Role of NADPH oxidase in H9c2 cardiac muscle cells exposed to simulated ischaemia-reperfusion

Elisabetta Borchi [a], Matteo Parri [a], Laura Papucci [b], Matteo Becatti [a], Niccolò Nassi [c], Paolo Nassi [a], Chiara Nediani [a, *]

[a] Department of Biochemical Sciences, University of Florence, Florence, Italy
[b] Department of Experimental Pathology and Oncology, University of Florence, Florence, Italy
[c] Department of Pediatrics, University of Florence, Florence, Italy

Received: May 20, 2008; Accepted: August 18, 2008

## Abstract

Oxidative stress is associated with several cardiovascular pathologies, including hypertension, cardiac hypertrophy and heart failure. Although oxidative stress is also increased after ischaemia-reperfusion (I/R), little is known about the role and the activation mechanisms, in cardiac myocytes under these conditions, of NADPH oxidase, a superoxide-producing enzyme. We found that rat cardiac muscle cells (H9c2) subjected to an *in vitro* simulated ischaemia (substrate-free medium plus hypoxia) followed by 'reperfusion', displayed increased reactive oxygen species (ROS) production attributable to a parallel increase of NADPH oxidase activity. Our investigation on mechanisms responsible for NADPH oxidase activation showed a contribution of both the increase of NOX2 expression and $p47^{phox}$ translocation to the membrane. We also found that the increase of NADPH oxidase activity was associated with higher levels of lipid peroxidation, the activation of redox-sensitive kinases, in particular ERK and JNK, and with cell death. Diphenyleneiodonium (DPI), a flavoprotein inhibitor used as NADPH oxidase inhibitor, prevented I/R-induced ROS formation in treated cells, together with the related lipoperoxidative damage, and JNK phosphorylation without affecting ERK activation, resulting in protection against cell death. Our results provide evidence that NADPH oxidase is a key enzyme involved in I/R-induced oxidant generation and suggest it can be a possible target in cardioprotective strategies against I/R injury, a condition of great importance in human pathology.

**Keywords:** NADPH oxidase • cardiac myocytes • simulated ischaemia-reperfusion • ROS • MAPK

## Introduction

It is widely recognized that the increased production of oxygen-derived radical species is a key event involved in cardiovascular pathologies, including hypertension, cardiac hypertrophy and heart failure [1–3]. Oxidative stress is also implicated in the metabolic and functional alterations associated with ischaemia-reperfusion (I/R) injury [4, 5]. The activation of enzymes such as xanthine oxidase or the uncoupling of the mitochondrial electron transport chain are believed to play an important role in reactive oxygen species (ROS) production [6, 7]. Recent studies have suggested NADPH oxidase as a major cardiovascular ROS source, whose activity appears enhanced by several stimuli relevant to vascular and heart disease, such as angiotensin II, norepinephrine and TNFα [8, 9]. NADPH oxidase is a multimeric enzyme that contains a core membrane-bound flavocytochrome comprising a catalytic NOX subunit and a lower molecular weight $p22^{phox}$ subunit. So far, five NOX isoforms (NOX1–5) have been identified in different tissues [10, 11]. NOX2 and NOX4, the main isoforms expressed in cardiac cells [12–14], are subjected to a different biochemical regulation. At variance with NOX4, NOX2 (or $gp91^{phox}$) activation requires the association of cytosolic regulatory subunits ($p47^{phox}$, $p67^{phox}$, $p40^{phox}$ and Rac1) [8]. The increase in subunits expression and/or the translocation of regulatory subunits (in particular $p47^{phox}$) from the cytosol to the membrane represent prerequisites for NOX2 activation and ROS production [8, 15–17]. NADPH oxidase activity and subunits expression are increased in experimental models of pressure overload left ventricular hypertrophy [13, 16]. Recently, we found that the NADPH oxidase activity was increased in the left and right ventricle of myocardium of patients with end-stage heart failure, and that this increase was associated with

*Correspondence to: Chiara NEDIANI,
Department of Biochemical Sciences, Viale Morgagni,
50 - 50134 Firenze, Italy.
Tel.: +390554598321
Fax: +390554598905
E-mail: chiara.nediani@unifi.it

doi:10.1111/j.1582-4934.2008.00485.x

$p47^{phox}$ translocation [18]. Instead, no convincing evidence on the role of cardiomyocyte NADPH oxidase in I/R has been reported.

ROS arising from the NADPH oxidase activity appear involved in modulating redox-sensitive signalling pathways, such as mitogen-activated protein kinase (MAPK) [8]. They consist of three major subfamilies: the extracellular signal-regulated kinase (ERK), mainly implicated in cell survival and proliferation [19, 20], as well as p38 and c-jun $NH_2$-terminal kinase (JNK), both related to cell death [21–23]. However, the exact role of the NADPH oxidase in signal-transduction remains largely unknown.

In the present study, the I/R was simulated in H9c2 cardiomyoblasts, a cell line extensively used in cardiological research since it shares most of the molecular and functional features of adult cardiomyocytes [24].

The aims of our investigation were the following: (1) investigating the role played by NADPH oxidase in cardiac cells exposed to simulated ischaemia/'reperfusion'; (2) assessing whether NADPH oxidase-derived ROS are involved in the activation of redox-sensitive signalling pathways; (3) describing the possible role performed by members of the MAPK family in cell death; (4) checking whether cardiomyocyte damage can be prevented by the use of NADPH oxidase (and MAPK) inhibitor(s).

# Materials and methods

## Cell cultures

Embryonic rat cardiomyoblasts (line H9c2 (2–1), n° 88092904) were provided from European Collection of Cell Cultures (ECACC, Salisbury, UK). H9c2 cells were plated at a density of $5 \times 10^5$/ 100 mm plate and cultured at 37°C in 5% $CO_2$ humidified atmosphere in Dulbecco's Modified Eagles Medium (DMEM, Sigma, Italy) supplemented with 10% heat-inactivated foetal bovine serum (FBS), 1% L-glutamine, 1% streptomycin and 1% penicillin. Cells were passaged regularly and sub-cultured to about 70–80% before experimental procedures.

## Experimental protocol

Simulated ischaemia was obtained as previously reported [25] with minor modifications. Briefly, H9c2 cells were cultured in a low volume of substrate-free medium (serum-free, glucose-free and sodium pyruvate-free DMEM, DME base, Sigma, Italy) into an anaerobic Plexiglas chamber (Billups-Rothenberg Inc., CA, USA), saturated with 95% $N_2$ and 5% $CO_2$, at 37°C for 24 hrs. The volume of hypoxic medium used was the minimum volume required to coat the cellular monolayer for the prevention of cellular dehydration during the ischaemic period. Simulated ischaemia was followed by a simulated 'reperfusion' period during which the cells were exposed to normoxic fresh culture medium at 37°C for 60 min. in the absence and in the presence of the following drugs: 10 μM diphenyleneiodonium chloride (DPI, Sigma, Italy), a flavoprotein inhibitor, and 100 μM apocynin (Sigma, Italy), both ones used as NADPH oxidase inhibitors, 10 mM 4,5-dihydroxy-1,3-benzene-disulfonic acid (Tiron, Sigma, Germany), a superoxide scavenger, 10 μM rotenone (Sigma, Italy), a mitochondrial oxidase complex I inhibitor, 100 μM oxypurinol (Sigma, Italy), a xanthine oxidase inhibitor, and 20 μM SP600125 (Sigma, Italy), a selective JNK inhibitor compound. Since some of these compounds were dissolved in dimethyl sulphoxide (DMSO), the same amount of the drugs was added to control cells to evaluate their possible toxic effects (data not shown).

## Sample preparation and protein content measurement

At the end of 'reperfusion', cells were washed with ice-cold PBS, harvested with a 0.25% Trypsin-EDTA solution, lysed in an ice-cold lysis buffer (10 mM Tris HCl, pH 7.4 containing 150 mM NaCl, 2 mM EGTA, 2 mM DTT, 10 μg/ml leupeptin, 10 μg/ml aprotinin, 1 mM PMSF and phosphatase inhibitor cocktail) for 60 min. and sonicated three times on ice for an overall 15 sec. time period. Then the samples were centrifuged at 3000 rpm at 4°C, and the supernatants were assayed for protein concentration by bicinchoninic acid (BCA) protein assay (Pierce, Italy), superoxide production, lipid peroxidation and subjected to Western blotting. To evaluate NOX2 ($gp91^{phox}$) protein expression and $p47^{phox}$ translocation, membrane and cytosolic fractions of the homogenates were separated by ultracentrifugation at 100,000× *g* for 60 min. at 4°C, and used for immunoblotting. The 'purity' of membrane and cytosolic fractions were confirmed by marker enzyme activities as previously described [26].

## Measurement of intracellular ROS

Intracellular ROS content was measured by monitoring the oxidation of 10 μM 2′, 7′-dihydrodichlorofluorescein diacetate ($H_2$DCF-DA, Invitrogen, Italy), a cell permeable compound, to fluorescent dichlorofluorescein as described previously [27]. Briefly, the cells, cultured in a 6-well plate, were treated with 10 μM $H_2$DCF-DA 10 min. before the end of reperfusion. After PBS washing, the cells were lysed in lysis buffer and immediately analysed on Fluoroskan Ascent Fluorometer (Thermo Electron Corporation, Finland). DCF fluorescence was expressed as arbitrary units (A U) and normalized to the total protein content.

## Superoxide production assay

Superoxide production was assessed by lucigenin-enhanced chemiluminescence as described previously [18]. Experiments were performed on a luminometer (Lumat LB 9507 EG&G Berthold) using 0.1 mg lysed cell protein/tube and a non-redox–cycling 5 μM lucigenin concentration. Superoxide generation was measured at room temperature in the absence or in the presence of the substrates of either the NADPH oxidase (0.3 mM NADPH), the mitochondrial oxidase complex I (5 mM succinate) or the xanthine oxidase (1 mM xanthine), respectively. Further measurements were taken after the addition of the oxidase inhibitors: diphenyleneiodonium (10 μM DPI), a flavoprotein inhibitor used as NADPH oxidase inhibitor, rotenone (50 μM), a mitochondrial oxidase complex I inhibitor or oxypurinol (100 μM), a xanthine oxidase inhibitor. A cell-permeable superoxide scavenger 4,5-dihydroxy-1,3-benzene-disulfonic acid (Tiron, 20 mM) was also used. A buffer blank was subtracted from each reading. Superoxide production was expressed as mean arbitrary light units per mg protein per sec. over a 10-min. period.

## Lipid peroxidation assay

To assess the level of lipid peroxidation, malondialdehyde (MDA) content was determined using a 'Biooxytech LPO-586 Assay' kit (Oxis International Inc., Prodotti Gianni, Italy).

## Western blotting

Equal protein amounts of lysed cell homogenate, membrane or cytosolic proteins were separated on 12% SDS-PAGE and transferred to polyvinylidene difluoride (PVDF) membranes. After blocking with 5% (w/v) BSA in 0.1% (v/v) PBS-Tween, the membranes were incubated overnight at 4°C with goat-anti-NOX2(gp91$^{phox}$) (1:1000, sc-5827), and goat anti-p47$^{phox}$ antibodies (1:1000, sc-7660) (Santa Cruz Biotechnology, Santa Cruz, CA, USA). $\alpha$-actin, detected with mouse monoclonal antibody (1:1000, sc-32251), was used as a loading control and HL-60 cell lysate (sc-2209) as a positive control for the detection of NOX2 (Santa Cruz Biotechnology).

MAPK activation was assessed by Western blotting using rabbit monoclonal antibodies that specifically recognize the phosphorylated active forms of these kinases (1:1000, #9938 Phospho- MAPK family kit, Cell Signaling Technology, MA, USA). The results are expressed relative to their total protein content, detected with rabbit polyclonal anti-JNK (1:1000, sc-571), anti-ERK (1:1000, sc-93) and anti-p-38 (1:1000, sc-535) antibodies (Santa Cruz Biotechnology). Anti-goat (1:3000, sc- 2020) or anti-rabbit (1:10000, sc- 2004) and anti-mouse (1:5000, sc- 2005) peroxidase-conjugated antibodies were used (Santa Cruz Biotechnology).

Immunoreactive bands were detected by chemiluminescence Super Signal West Dura solution (Pierce, Italy) and quantified by densitometry analysis using a Chemi Doc system and Quantity One software (Bio-RAD Laboratories, Italy).

## Immunofluorescence analysis for NOX2 protein expression and p47$^{phox}$ membrane translocation

For immunofluorescence staining, H9c2 cells were grown on coverslips (VWR, Strasbourg, France) in 35-mm culture dishes (Barloworld Sci, Milan, Italy). After I/R, cells were fixed with 3% (v/v) paraformaldheyde/PBS for 20 min. at 4°C, permeabilized with 0.1% (v/v) Triton-X-100/TBS and blocked with PBS containing 1% BSA and 10% horse serum for 60 min. The coverslips were incubated overnight at 4°C with 1:50 goat-anti-NOX2 (gp91$^{phox}$) or goat-anti-p47$^{phox}$ antibodies dissolved in TBS containing 3% BSA. After washing three times in 0.1% Triton-X-100/TBS and once with 0.1% BSA in 0.1% Triton-X-100/TBS, a 1:400 fluorescein-isothiocyanate (FITC)-conjugated anti-goat secondary antibody (green fluorescence, Fluka, Switzerland) was added for 60 min. After several washes in 0.1% Triton-X-100/TBS the cell nuclei were stained with a propidium iodide solution (Fluka, Switzerland). Coverslips were aspirated dry, sealed with glass slides in Gel Mount (Sigma, Italy) and observed by a TCS-SP5 confocal microscopy (Leica Microsystems, Germany), performed with a 488 nm argon ion laser line for FITC excitation.

## Cell death assessment

Cell viability was determined by Trypan blue (TB) dye uptake. Cells were gently harvested and mixed with 0.4% TB solution (Sigma, Italy) and the resulting cell suspension was counted under a phase-contrast inverted microscope. The viable cells with intact cell membranes, which were able to exclude the dye, were counted using a haemocytometer and expressed as percentage over the total cell counted (cell viability).

Lactate dehydrogenase (LDH) release into the culture medium, a marker of cell mortality, particularly of necrotic death, was determined by using a cytotoxicity detection kit (Promega, USA). LDH release was calculated with respect to the total LDH content measured after complete cell lysis by 1% Triton-X-100.

## Statistical analysis

All values are expressed as mean ± S.E.M. Comparisons were performed using ANOVA followed by a Tukey–Kramer multiple comparison test. Correlation coefficient $r$ was obtained using a linear (Pearson) correlation test. Probabilities of $P \leq 0.05$ were considered statistically significant.

# Results

## Simulated I/R increases intracellular ROS production

Cells subjected to simulated I/R showed a significant increase in intracellular ROS production examined by $H_2$DCF-DA fluorescence intensity compared with normoxic controls (Fig. 1). To determine the source of ROS generation, we examined the effects of a flavoprotein inhibitor DPI and apocynin, both compounds being commonly used as NADPH oxidase inhibitors [11], of the mitochondrial oxidase complex I inhibitor, rotenone, and of the xanthine oxidase inhibitor, oxypurinol. DPI and apocynin treatment induced a significant decrease of fluorescence, although apocynin exerted its inhibitory effect at a higher concentration compared with DPI. Albeit not sufficient to restore completely the conditions of normoxic control cells, both compounds reduced ROS production to a value similar to that obtained with the superoxide scavenger Tiron. Rotenone and oxypurinol had no effect on I/R-induced ROS generation .

## Effect of simulated I/R on NADPH oxidase activity

To confirm that simulated I/R-induced ROS production was mainly attributable to the activation of NADPH oxidase, experiments were performed in the absence and in the presence of specific oxidase substrates and superoxide production was measured by lucigenin chemiluminescence. In the presence of succinate or xanthine, substrates of the mitochondrial oxidase complex I and of the xanthine oxidase, respectively, $O_2^{\cdot -}$ production was minimal in I/R cells (Fig. 2A). On the contrary, significantly higher $O_2^{\cdot -}$ generation was detected in I/R cells in the presence of NADPH compared with I/R cells without substrate. The increase of NADPH-dependent superoxide production was significantly inhibited by DPI and Tiron

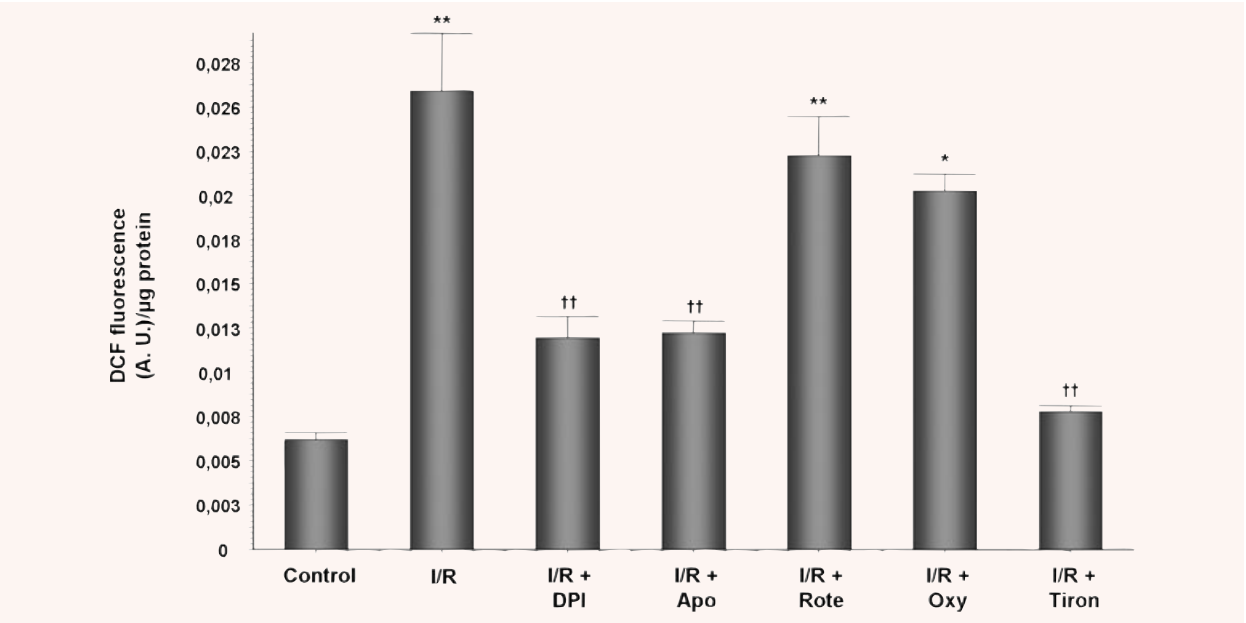


**Fig. 1** Effects of oxidase inhibitors on intracellular ROS formation in H9c2 cardiac muscle cells exposed to simulated ischaemia followed by reperfusion. DCF fluorescence is expressed as arbitrary units (AU) normalized to cellular protein content. Values are means ± S.E.M.; DPI, a flavoprotein inhibitor; Apocynin (Apo), an NADPH oxidase inhibitor; Rotenone (Rote), a mitochondrial oxidase complex I inhibitor; Oxypurinol (Oxy), a xanthine oxidase inhibitor; Tiron, a superoxide scavenger, used as a control. $^{*}P < 0.05$ and $^{**}P < 0.01$ *versus* control (normoxic condition); $^{\dagger\dagger}P < 0.01$ *versus* I/R; $n = 6$, separate cell cultures.

(Fig. 2B), but was unaffected by rotenone or oxypurinol, supporting NADPH oxidase as the likely major source of $O_2^{\cdot-}$ in cells exposed to simulated I/R.

## Effect of simulated I/R on NOX2 and p47$^{phox}$ expression

To elucidate the mechanisms underlying NADPH oxidase activation in cells subjected to simulated I/R, we analysed the expression of the catalytic subunit NOX2 by Western blot and immunofluorescence. As shown in Fig. 3A, immunoblotting of NOX2 membrane protein expression with a goat polyclonal antibody, widely used by other authors [28–30], gave two different bands that migrated at a position of approximately 55–65 kD. These bands presumably represented unglycosylated NOX2 [31], whereas no band was detected around 80 kD probably representing glycosylated NOX2. Notwithstanding the molecular properties of NOX2 detected by the antibody, it is evident that both bands are more intense in I/R samples with respect the control, thus suggesting an effective overexpression of NOX2 protein after I/R. DPI addition had no effect on NOX2 expression. The increase in NOX2 expression was further confirmed by immunofluorescence (Fig. 3B). In control H9c2 cells confocal images showed that NOX2 expression was localized in plasma membrane and in the cytosol including the perinuclear region (Fig. 3B-a). After simulated I/R NOX2 labelling appeared more intense and showed a vesicular or granular pattern in all these compartments (Fig. 3B-b), that was not modified by DPI treatment (Fig. 3B-c). To assess whether NADPH oxidase activation in cells exposed to simulated I/R-matched p47$^{phox}$ overexpression and/or translocation, we undertook immunofluorescence staining. As shown in Fig. 4A, p47$^{phox}$ expression was enhanced in I/R H9c2 compared with control cells; moreover, the cellular location of the labelling appeared increased in the cytosol and especially in the plasma membrane. Treatment with DPI resulted in a decreased p47$^{phox}$ immunofluorescence staining, which was mainly evident in the sarcolemma, suggesting a change in p47$^{phox}$ distribution and supporting the hypothesis of a p47$^{phox}$ translocation from the cytosol to plasma membrane. To confirm these data, we analyse p47$^{phox}$ content in the membrane and cytosolic fractions by Western blotting. Figure 4B shows a significantly higher membrane/cytosolic ratio of p47$^{phox}$ than in controls; DPI treatment abolished this increase (Fig. 4). These results underscore that, in our experimental conditions, the increase in NADPH oxidase activity is due not only to NOX2 overexpression but also to translocation of the cytosolic subunit p47$^{phox}$ to the membrane.

## Lipid peroxidation

Lipid peroxidation resulting from oxidative stress has been implicated in cell death. To test whether simulated I/R-mediated NADPH

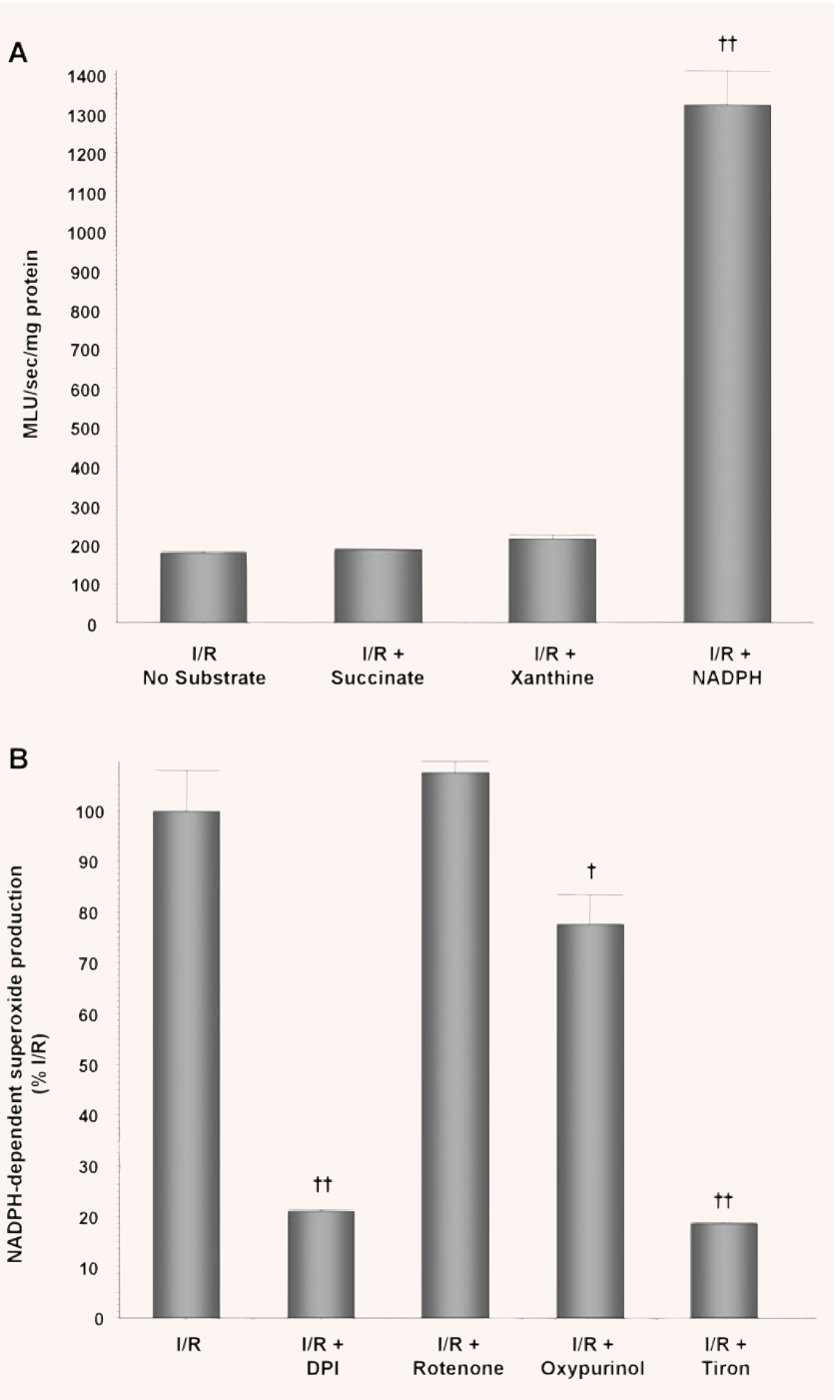


**Fig. 2** Superoxide production in ischaemic-reperfused (I/R) H9c2 homogenate in response to several substrates (**A**) and NADPH-dependent superoxide production in the absence and in the presence of oxidase inhibitors (**B**) detected by lucigenin chemiluminescence. Results are expressed as MLU per sec. per mg protein. Values are means ± S.E.M.; NADPH, NADPH oxidase substrate; succinate, mitochondrial oxidase complex I substrate; xanthine, xanthine oxidase substrate. MLU, mean arbitrary light units. $^{\dagger}P < 0.05$ and $^{\dagger\dagger}P < 0.01$ *versus* I/R; $n = 6$, separate cell cultures.

oxidase activation was involved in lipoperoxidative cell damage, we measured MDA cell content as an indirect index of ROS activity in the absence and in the presence of DPI. Consistent with the differences observed in ROS production, MDA levels were significantly increased in cells subjected to simulated I/R. In the presence of DPI, MDA content was significantly reduced, as we observed with Tiron treatment (Fig. 5), suggesting that NADPH oxidase-derived ROS is mainly responsible for oxidative stress damage in I/R cells.

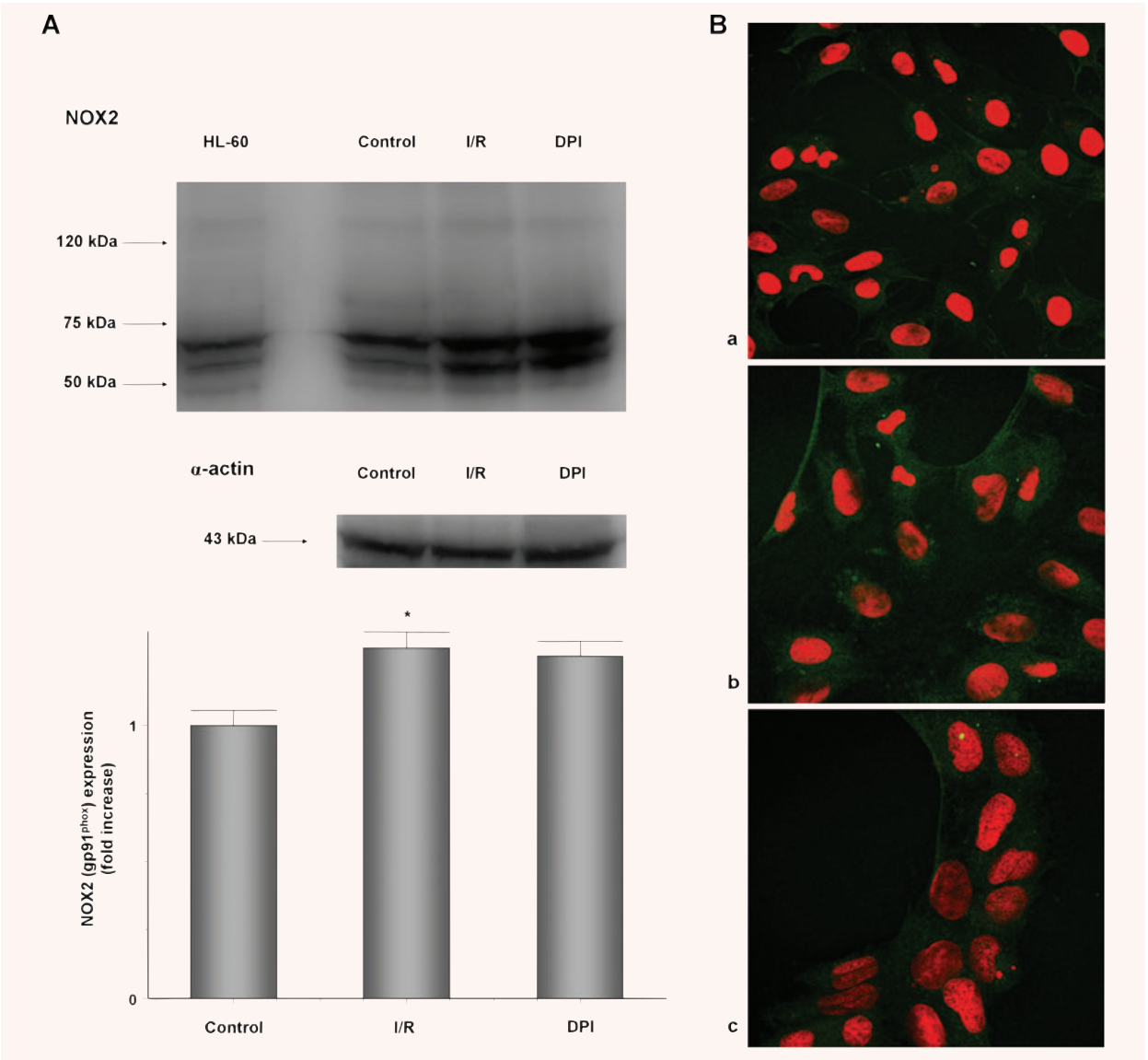


**Fig. 3** Changes in NOX2 ($gp91^{phox}$) protein expression in H9c2 cardiac muscle cells subjected to simulated ischaemia and reperfusion in the absence and in the presence of DPI. (**A**) Representative immunoblot of NOX2 (upper) and densitometric quantification of NOX2 membrane expression level (relative to α-actin, used as a loading control) (lower), expressed as fold increase of control. HL-60 cell lysate was used a positive control for the detection of NOX2. Values are means ± S.E.M.; * $P < 0.05$ *versus* control; $n = 6$, separate cell cultures (**B**) Confocal images of (a) control, (b) I/R and (c) DPI-treated I/R H9c2 cells. The cells were fixed and processed as described in Materials and Methods.

## MAPK activation

To elucidate the signal transduction pathway involved in simulated I/R injury, we evaluated the level of phosphorylation of the three principal members of the MAPK family (p38, ERK and JNK) by Western blotting. In cells exposed to simulated I/R, no significant difference were found in the p38 phosphorylation status (expressed as p-p38/p-38 ratio) with respect to control cells (Fig. 6A), whereas ERK (p-ERK/ERK ratio) and JNK (p-JNK/JNK ratio) phosphorylation were significantly increased (1.7-fold, $P < 0.01$; and 2-fold, $P < 0.05$; both *versus* control; Fig. 6B and C).

In order to verify a possible link of these events with the NADPH oxidase activation, we analysed ERK and JNK phosphorylation in the presence of DPI. DPI treatment decreased significantly only the p- JNK/JNK ratio; similarly, the selective JNK inhibitor,

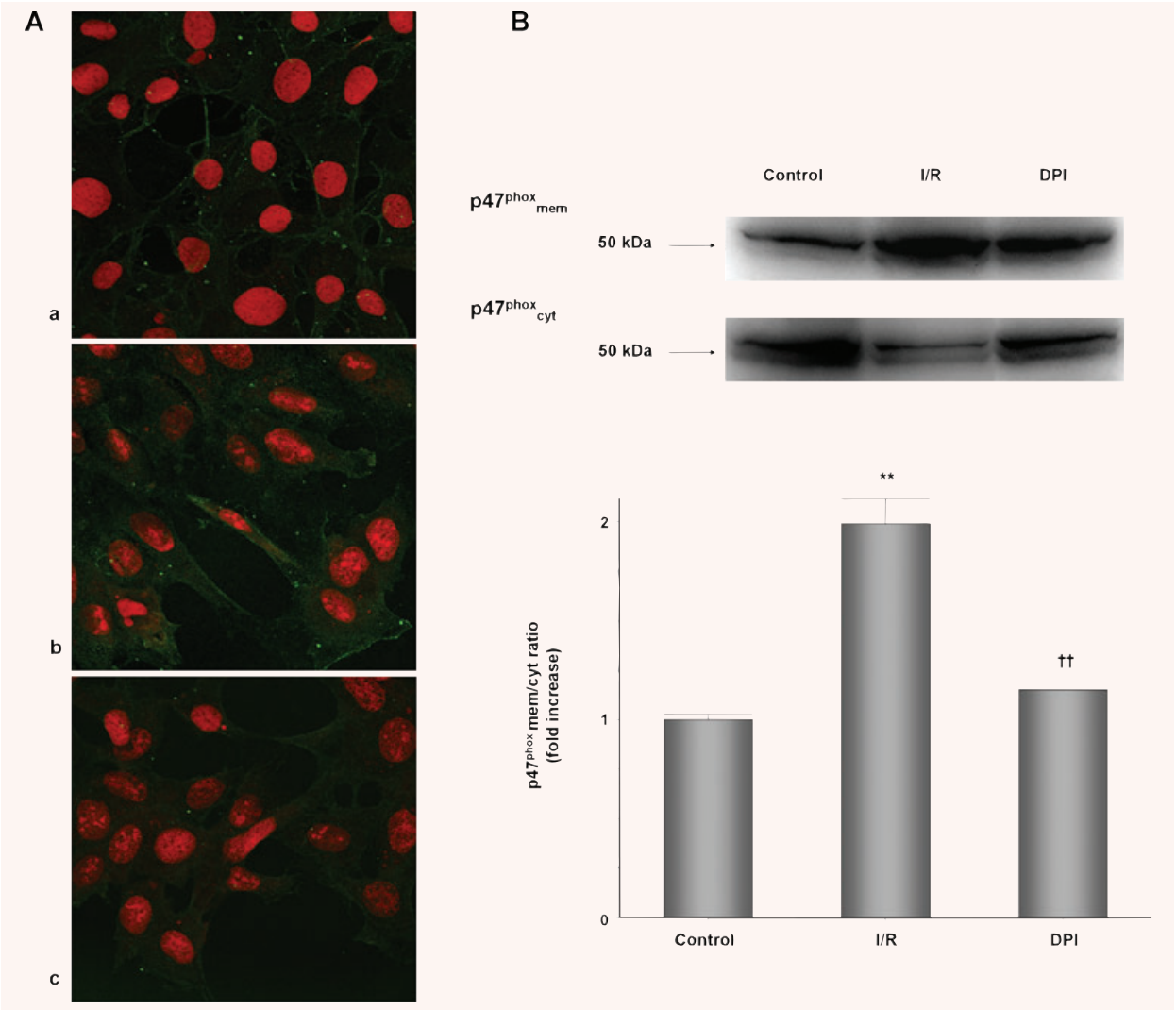


**Fig. 4** p47$^{phox}$ membrane translocation in H9c2 cardiac muscle cells following simulated ischaemia and reperfusion in the absence and in the presence of DPI. (**A**) Immunofluorescence of (a) control, (b) I/R and (c) DPI-treated I/R H9c2 cells. (**B**) Representative immunoblots of p47$^{phox}$ protein expression of membrane and cytosolic fraction of H9c2 cardiac muscle cells (upper). Densitometric quantification of the ratio of membrane to cytosolic protein expression of p47$^{phox}$ (lower). Values are means ± S.E.M. $^{**}P < 0.01$ *versus* control; $^{††}P < 0.01$ *versus* I/R; $n = 6$, separate cell cultures.

SP600125, reduced the p- JNK/JNK ratio to control level [32] (Fig. 6). In agreement with this effect, a positive correlation ($r = 0.74$, $P < 0.01$) was found between NADPH oxidase-derived superoxide production and JNK activation.

## Cell viability and LDH release

As judged by the Trypan blue exclusion assay (Fig. 7A), the viability of cells submitted to I/R was decreased by 26% with respect to the controls. Accordingly, the fraction of total LDH released in the culture medium (Fig. 7B) by I/R cardiomyoblasts was significantly increased (1.6-fold, $P < 0.05$ *versus* control). All these effects were significantly reduced by the treatment with the two unrelated inhibitors DPI or SP600125; in fact, cell treatment with both inhibitors resulted in the same protective effect against simulated I/R-induced cell death. Moreover, the percentage of both viable cells and released to total LDH showed a significant correlation ($r = –0.73$, $P < 0.01$ and $r = 0.75$, $P < 0.01$, respectively) with JNK phosphorylation.

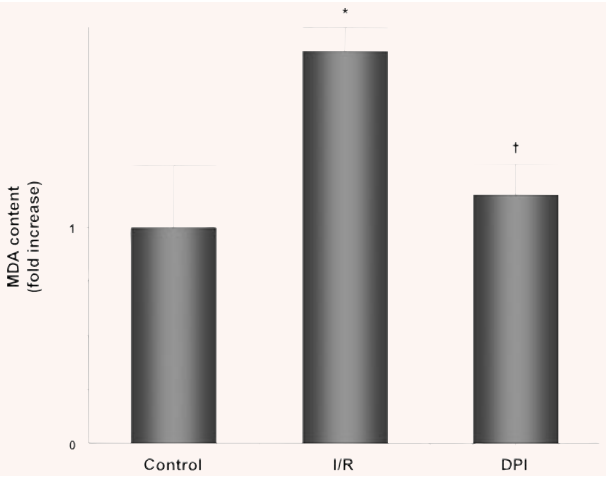


**Fig. 5** Lipid peroxidation, assessed as intracellular MDA content, in H9c2 cardiac muscle cells subjected to simulated ischaemia followed by reperfusion in the absence and in the presence of DPI . Values are expressed as fold increase of control. $^{*}P < 0.05$ *versus* control; $^{\dagger}P < 0.05$ *versus* I/R; $n = 6$, separate cell cultures.

## Discussion

The novel finding in this study is that the production of NADPH oxidase-derived ROS was enhanced in cardiomyoblasts maintained for 24 hrs under ischaemia-simulating conditions followed by 1 hr of simulated 'reperfusion'. This was accompanied by increases in lipid peroxidation, in activation of specific redox-sensitive kinases and cell death. Inhibition of NADPH oxidase activity by the flavoenzyme inhibitor DPI largely prevented simulated I/R-induced ROS formation; the latter matched a reduction in MDA content, a significant decrease in p-JNK/JNK ratio and an evident protection against cell death.

The main aim of our study was to describe the role of NADPH oxidase in cardiac cell exposed to simulated I/R. In fact, albeit several recent studies have examined the influence of myocardial I/R on NADPH oxidase, there are only few and conflicting data about the contribution of this oxidase complex to I/R-cell damage and its regulation. The present investigation follows our previous demonstration that, in the myocardium from end-stage ischaemic and non-ischaemic cardiomyopathy, an increased NADPH oxidase activity was significantly related with enhanced lipid peroxidation and activation of redox sensitive kinases. The limitation on finding a clear evidence for a cause–effect relationship in end-stage hearts [18] is the reason for using H9c2 cardiomyoblasts line in the present study. This cell line, sharing features of adult cardiomyocytes [24], is considered a valuable model for mechanicistic studies aimed to investigate the pathways implicated in cardiac cell death following oxidative stress [33]. Previous works in this area include studies of oxidative cell damage caused by doxorubicin [33, 34], hydrogen peroxide [35] and ischaemia/reperfusion [36, 37]. As indicated in the section 'Materials and Methods', we subjected H9c2 to an *in vitro* simulated ischaemia for 24 hrs followed by 1 hr of simulated 'reperfusion'. In this connection, several reports have documented the need for long-term hypoxia (24–72 hrs) for the appearance of evident damages in primary cultures of neonatal rat cardiac myocytes [37–39], a finding that suggests the presence of intrinsic mechanisms in cardiac myocytes protecting these cells from hypoxia-related injury. Unpublished data from our laboratory confirmed a similar behaviour also for H9c2 cardiomyoblasts, indicating 24 hrs of simulated ischaemia followed by 1 hr of 'reperfusion' as the optimal experimental condition to obtain significant alterations in this cell line.

Potential sources of oxidative stress during I/R include mitochondria, NADPH oxidase and xanthine oxidase [6–8, 11]. However, a comprehensive understanding of the relative contributions of these systems during I/R has not yet emerged. In the present study, cardiomyoblasts exposed to simulated I/R conditions showed an increased intracellular ROS production that, as indicated by DCF fluorescence, was remarkably suppressed by the superoxide scavenger Tiron. A similar significant reduction was obtained with apocynin, widely considered as a specific NADPH oxidase inhibitor, and DPI, a potent flavoprotein inhibitor non-specific for NADPH oxidase but commonly used as a NOX inhibitor [11]. On the other hand, rotenone, a specific mitochondrial oxidase inhibitor and oxypurinol, a xanthine oxidase inhibitor, appeared to fail in reducing ROS production. These findings suggest that, under our simulated I/R conditions, superoxide was the main ROS produced and NADPH oxidase was its major source, although other contribution in ROS generation cannot be ruled out. The prominent role of NADPH oxidase in superoxide generation was confirmed by lucigenin chemiluminescent measurements showing that NADPH, but not other added substrates, increased the capacity of cardiomyoblasts exposed to simulated I/R to produce such free radical.

Previous investigations in cell and animal models highlighted that NADPH oxidase activation occurs through either increased expression or post-translational modifications and translocation of the oxidase subunits [8, 15, 17, 40]. Recent studies have reported in H9c2 cell line the presence of the NOX2 ($gp91^{phox}$) isoform previously identified in human cardiomyocytes [41]. We confirmed this finding and, in addition, we found that the same cells subjected to simulated I/R showed an increased expression of NOX2 ($gp91^{phox}$); this effect occurred in parallel with an apparent translocation of $p47^{phox}$ from the cytosol to the membrane, as shown by a significant increase of the $p47^{phox}$ membrane/cytosol ratio. Serine phosphorylation of $p47^{phox}$ by protein kinase C (PKC) appears to be the prerequisite for $p47^{phox}$ translocation and stable interaction with membrane-bound cytochrome $b_{558}$ resulting in oxidase activation [40]. It is well known that many stimuli, such as angiotensin II or TNF-$\alpha$, can increase NADPH oxidase activity by PKC activation [40, 42]. PKCs are also important for stress responses in various tissues and PKC$\varepsilon$ is the primary PKC isoform that is affected by hypoxia or ischaemia in heart muscle [43, 44]. Recently, some authors have shown that the addition of chelerythrine, a broad spectrum PKC inhibitor, or apocynin, a NADPH

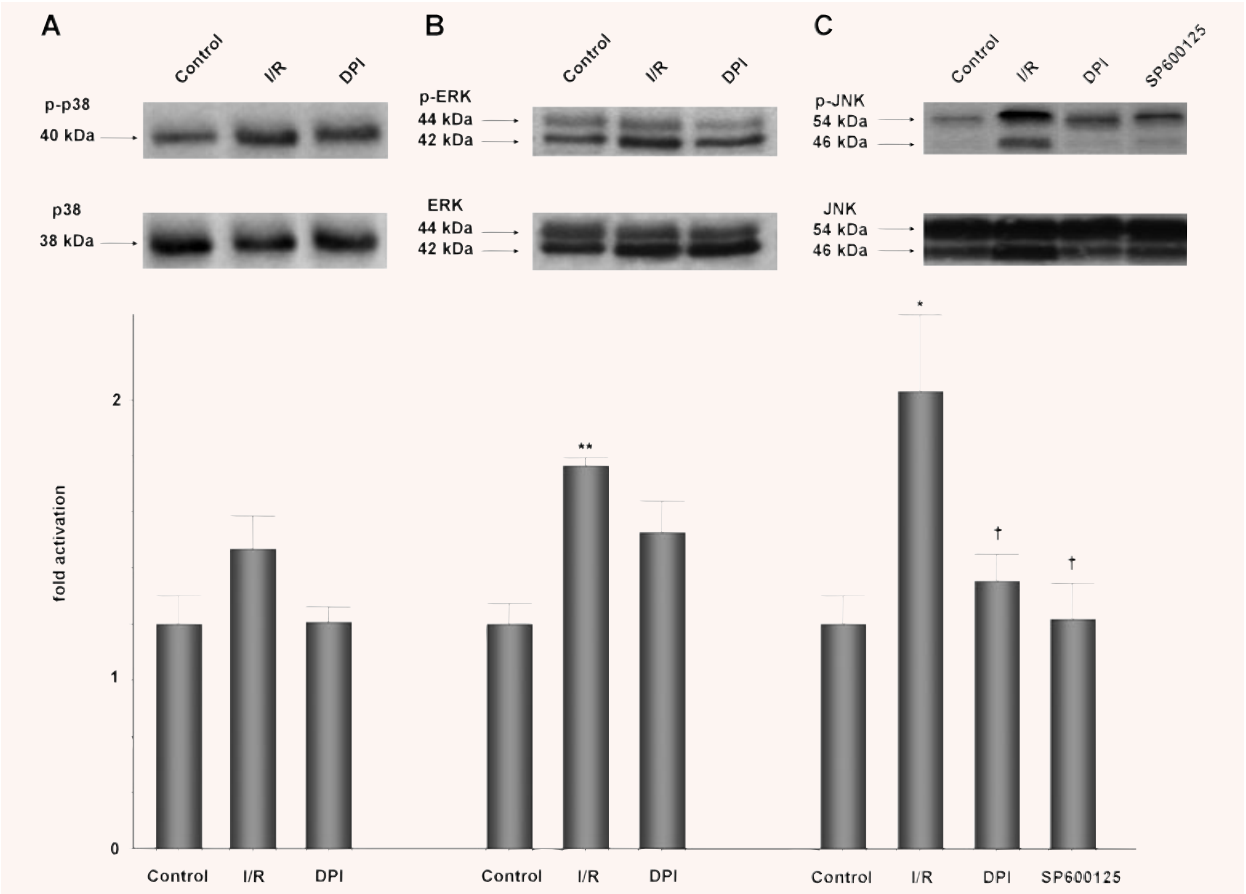


**Fig. 6** Effect of DPI (**A**, **B**, **C**) and of SP600125 (**C**) on MAPKs activation induced by simulated ischaemia and reperfusion in H9c2 cardiac muscle cells. Representative immunoblots for p-p38 (**A**), p-ERK (**B**) and p-JNK (**C**) (upper) and respective total protein in H9c2 homogenate (lower). Densitometric quantification of ratio of phosphorylated to total protein of MAPKs expressed as fold activation relative to control. SP600125, selective JNK inhibitor compound. $^{*}P < 0.05$ and $^{**}P < 0.01$ *versus* control; $^{\dagger}P < 0.05$ *versus* I/R; $n = 6$, separate cell cultures.

oxidase inhibitor, before reoxygenation of anoxic endothelial cells, decreased $O_2^{\cdot -}$ production to comparable levels, indicating that NADPH oxidase activation is PKC-dependent [45]. It seems reasonable that also in our experimental model the activation of PKC induces $p47^{phox}$ phosphorylation, its subsequent translocation to the membrane and interaction with membrane-bound cytochrome $b_{558}$ followed by the increased production of oxidant species. Recent studies reported that ischaemia resulted in NOX2 up-regulation in H9c2 cells and that DPI had no effect on NOX2 expression [41]. In line with this finding, we found that DPI treatment did not decrease NOX2 expression in our cells exposed to simulated I/R, rather it reduced $O_2^{\cdot -}$ generation and $p47^{phox}$ translocation. Although it is generally accepted that DPI decreases NADPH oxidase-derived ROS production, a reduced $p47^{phox}$ translocation did not appear so obvious. To our knowledge, whereas it is recognized that the interaction of apocynin with the oxidase may form a structure that impedes the formation of the $p47^{phox}$ subunit-cytochrome $b_{558}$ assembly [46], no data exist about the mechanism by which DPI might interfere with $p47^{phox}$ binding to the oxidase complex. Apart from this aspect that needs further investigation, the above reported findings suggest that under our experimental conditions both the increase in NOX2 expression and $p47^{phox}$ translocation to the membrane contribute to the observed NADPH oxidase activation.

The ROS-mediated membrane lipid peroxidation has been proposed as a main chemical modification resulting in cell death [47]. Our cardiomyoblasts subjected to simulated I/R, in fact, displayed significant increases in lipid peroxidation, as shown by their MDA levels, and in cell death. Both these events were prevented by DPI treatment, which indicates, in agreement with previous findings [48, 49], NADPH oxidase-generated ROS as major contributors to the I/R-induced lipid peroxidation and the related effects, including cell death.

In this connection, although the downstream pathways through which NADPH oxidase activation could lead to cardiac cell death remain to be fully elucidated, it has recently been demonstrated

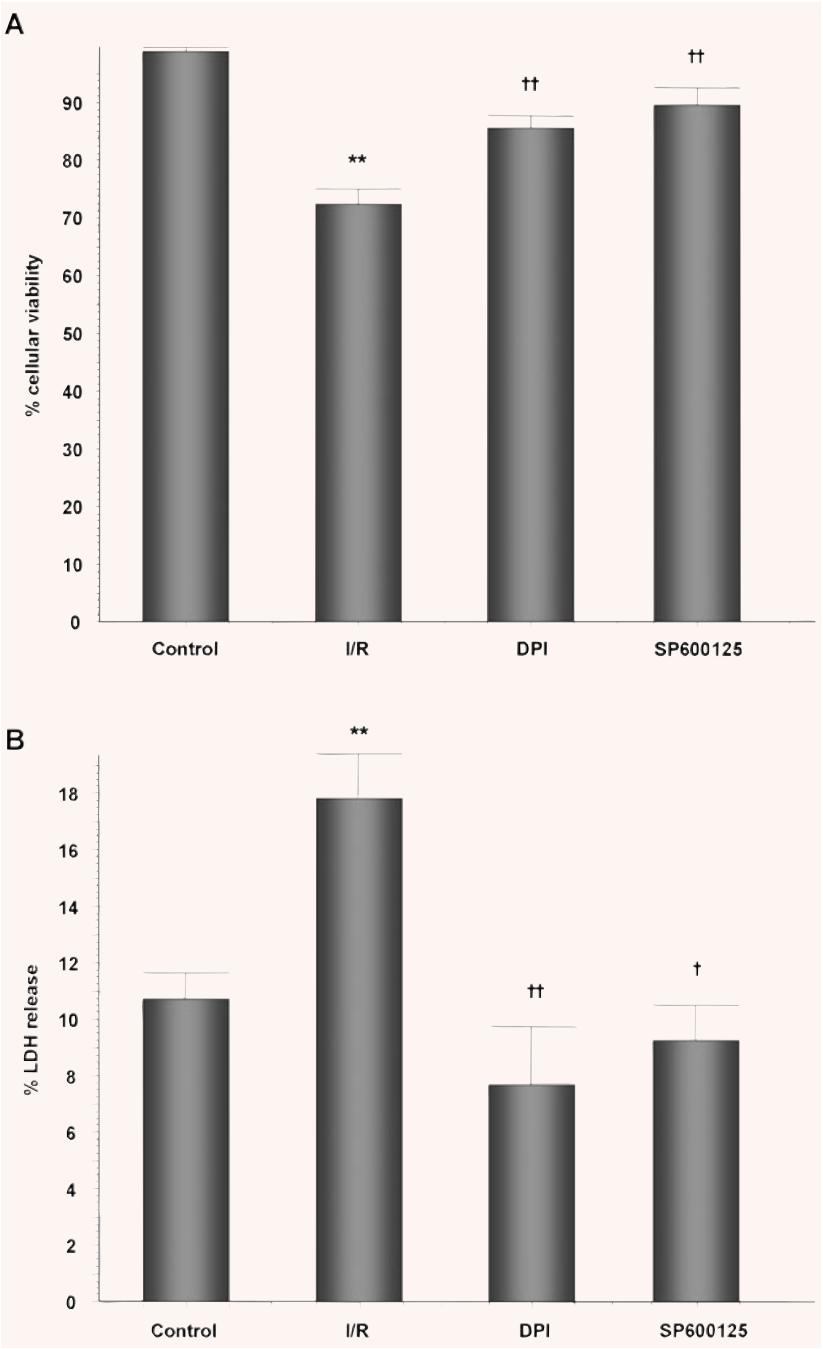


**Fig. 7** Effect of DPI and of SP600125 on cell death of H9c2 cardiac muscle cells exposed to simulated ischaemia and reperfusion. Cell death was evaluated by Trypan blue dye exclusion assay (**A**) and by LDH released into the culture medium (**B**). For Trypan blue assay, results are expressed as percentage of the viable cells over the total cell counted, respectively. For LDH release, results are expressed as percentage of total LDH content. $^{**}P < 0.01$ *versus* control; $^{\dagger}P < 0.05$ and $^{\dagger\dagger}P < 0.01$ *versus* I/R; $n = 6$, separate cell cultures.

that myocardial I/R activates MAPK subfamilies, including the 'stress-responsive' JNK and p38, both involved in cell death, and ERK, implicated in cell survival signalling [21, 22, 50]. However, p38 does not appear to be activated in all I/R models and some authors reported that during ischaemia the increase of p38 activity is initially rapid but subsequently declines rapidly [51]. In agreement with these observations, we did not find any modification of the p-p38/p38 ratio under our experimental conditions. Instead, we observed a significant activation of ERK and, to a higher extent, of JNK, whose phosphorylation was positively and significantly correlated with the cell death indexes. DPI treatment of I/R cardiomyoblasts did not affect p-ERK/ERK ratio, whereas it significantly decreased JNK phosphorylation, suggesting a different mechanism of I/R-induced activation for these two MAPKs. The

DPI effect on JNK activation was similar to that observed with SP600125, a specific inhibitor of JNK. Interestingly, these two unrelated inhibitors displayed a similar protective effect also in preventing I/R cell death. Taken together, these findings suggest that the NADPH oxidase-derived superoxide production plays a relevant role in JNK activation, as demonstrated by the positive and significant correlation between the two events. In turn, JNK activation appears to be determinant to induce the death of our cells exposed to simulated I/R. The simultaneous activation of this kinase and ERK is not surprising and many *in vivo* and *in vitro* studies reported a concomitant activation of these two kinases after hypoxia/ischaemia and reoxygenation [35, 52–54]. Moreover, when stimuli concomitantly activate multiple MAPKs the physiological response to stimulus will depend on the time course and strength of the signal. The balance between MAPK activation levels may influence cellular fate and turn towards cell death or life. In our experimental model, the concomitant activation of ERK and JNK might explain the moderate increase (about 26%) in cell death observed in our I/R cells. Moreover, the partial reduction of ERK phosphorylation following DPI treatment suggests that this process, at least in our experimental conditions, was activated by other factors in addition to oxidative stress.

I/R-triggered cardiomyocyte death can occur by either apoptosis or necrosis [55]. However, it should be considered that the mode of cell death resulting from I/R injury depends, to some extent, on the experimental conditions, and that necrosis and apoptosis represent only the extremes of a continuum of various modes of cell death. At any rate, we did not assess the relative incidence of these two forms of cell death, because this issue was beyond the scope of the present study.

In conclusion, the present study points out the NADPH oxidase as the critical enzyme that increases I/R-induced oxidant generation in cardiac cells and, at the same time, provides evidence for the mechanism of its activation. Furthermore, the inhibition of the NADPH oxidase by the flavoenzyme inhibitor DPI largely prevents I/R-induced lipoperoxidative damage and the activation of JNK pathway, associated to cell death, without affecting the ERK-related survival response.

We are conscious that this study was performed using both a non-contractile cell line, which poorly took account of the load factor, and an *in vitro* model of simulated ischaemia/reperfusion, which is devoid of any exogenous neuro-humoural influence. In spite of these limitations, the marked improvement of cell survival resulting from NOX inhibition in our experimental conditions stresses the importance to perform further investigation, including *in vivo* studies to outline cardioprotective strategies against I/R injury, a condition of great importance in the clinical setting.

## Acknowledgements

This work was supported by grants from the University of Florence (Fondi di Ateneo, ex 60%). We are grateful to Dr. Riccardo Favilli for his technical assistance and Prof. Cerbai for her critical review.

## References

1. **Sawyer DB, Siwik DA, Xiao L, *et al.*** Role of oxidative stress in myocardial hypertrophy and failure. *J Mol Cell Cardiol*. 2002; 34: 379–88.
2. **Cai H, Harrison DG.** Endothelial dysfunction in cardiovascular disease: the role of oxidant stress. *Circ Res*. 2000; 87: 840–4.
3. **Li JM, Shah AM.** Endothelial cell superoxide generation: regulation and relevance for cardiovascular pathophysiology. *Am J Physiol Regul Integr Comp Physiol*. 2004; 287: 1014–30.
4. **Becker LB, Vanden Hoek TL, Shao ZH, *et al.*** Generation of superoxide in cardiomyocytes during ischemia before reperfusion. *Am J Physiol Heart Circ Physiol*. 1999; 277: H2240–6.
5. **Becker LB.** New concepts in reactive oxygen species and cardiovascular reperfusion physiology. *Cardiovasc Res*. 2004; 61: 461–70.
6. **Meneshian A, Bulkley GB.** The physiology of endothelial xanthine oxidase: from urate catabolism to reperfusion injury to inflammatory signal transduction *Microcirculation*. 2002; 9: 161–75.
7. **Giordano FJ.** Oxygen, oxidative stress, hypoxia, and heart failure. *J Clin Invest*. 2005; 115: 500–8.
8. **Murdoch CE, Zhang M, Cave AC, *et al.*** NADPH oxidase-dependent redox signaling in cardiac hypertrophy, remodelling and failure. *Cardiovasc Res*. 2006; 71: 208–15.
9. **Murdoch CE, Grieve DJ, Cave AC, *et al.*** NADPH oxidase and heart failure. *Curr Opin Pharmacol*. 2006; 6: 1–6.
10. **Lambeth JD.** Nox enzymes, ROS, and chronic disease: an example of antagonistic pleiotropy. *Free Rad Biol Med*. 2007; 43: 332–47.
11. **Bedard K, Krause KH.** The NOX family of ROS-generating NADPH oxidases: physiology and pathophysiology. *Physiol Rev*. 2007; 87: 245–313.
12. **Li J, Stouffs M, Serrander L, *et al.*** The NADPH oxidase NOX4 drives cardiac differentiation: role in regulating cardiac transcription factors and MAP kinase activation. *Mol Biol Cell*. 2006; 17: 3978–88.
13. **Byrne JA, Grieve DJ, Bendall JK, *et al.*** Contrasting roles of NADPH oxidase isoforms in pressure-overload *versus* angiotensin II-induced cardiac hypertrophy. *Circ Res*. 2003; 93: 802–5.
14. **Bendall JK, Cave AC, Heymes C, *et al.*** Pivotal role of a gp91 phox-containing NADPH oxidase in angiotensin II-induced cardiac hypertrophy in mice. *Circulation*. 2002; 105: 293–6.
15. **Heymes C, Bendall JK, Ratajczak P, *et al.*** Increased myocardial NADPH oxidase activity in human heart failure. *J Am Coll Cardiol*. 2003; 41: 2164–71.
16. **Li JM, Gall NP, Grieve DJ, *et al.*** Activation of NADPH oxidase during progression of cardiac hypertrophy to failure. *Hypertension*. 2002; 40: 477–84.
17. **Li JM, Fan LM, Christie MR, *et al.*** Acute tumor necrosis factor alpha signaling *via* NADPH oxidase in microvascular endothelial cells: role of p47phox phosphorylation and binding to TRAF4. *Mol Cell Biol*. 2005; 25: 2320–30.
18. **Nediani C, Borchi E, Giordano C, *et al.*** NADPH Oxidase-dependent redox signaling in human heart failure: relationship

between the left and right ventricle. *J Mol Cell Cardiol*. 2007; 42: 826–34.

19. **Yue TL, Wang C, Gu JL, *et al.*** Inhibition of extracellular signal-regulated kinase enhances ischemia/reoxygenation-induced apoptosis in cultured cardiac myocytes and exaggerates reperfusion injury in isolated perfused heart. *Circ Res*. 2000; 86: 692–9.
20. **Nair VD, Yuen T, Olanow CW, *et al.*** Early single cell bifurcation of pro- and antiapoptotic states during oxidative stress. *J Biol Chem*. 2004; 279: 27494–501.
21. **Engelbrecht AM, Niesler C, Page C, *et al.*** p38 and JNK have distinct regulatory functions on the development of apoptosis during simulated ischaemia and reperfusion in neonatal cardiomyocytes. *Basic Res Cardiol*. 2004; 99: 338–50.
22. **Baines CP, Molkentin JD.** STRESS signaling pathways that modulate cardiac myocyte apoptosis. *J Mol Cell Cardiol*. 2005; 38: 47–62.
23. **Shen HM, Zheng LG.** JNK signaling pathway is a key modulator in cell death mediated by reactive oxygen and nitrogen species. *Free Rad Biol Med*. 2006; 40: 928–39.
24. **Hescheler J, Meyer R, Plant S, *et al.*** Morphological, biochemical, and electrophysiological characterization of a clonal cell (H9c2) line from rat heart. *Circ Res*. 1991; 69: 1476–86.
25. **Malliopoulou V, Xinaris C, Mourouzis I, *et al.*** High glucose protects embryonic cardiac cells against simulated ischemia. *Mol Cell Biochem*. 2006; 284: 87–93.
26. **Li JM, Shah AM.** Intracellular localization and preassembly of the NADPH oxidase complex in cultured endothelial cells. *J Biol Chem*. 2002; 277: 19952–60.
27. **LeBel CP, Ischiropoulos H, Bondy SC.** Evaluation of the probe 2′,7′-dichlorofluorescin as an indicator of reactive oxygen species formation and oxidative stress. *Chem Res Toxicol*. 1992; 5: 227–31.
28. **Gupte SA, Kaminski PM, Floyd B, *et al.*** Cytosolic NADPH may regulate differences in basal Nox oxidase-derived superoxide generation in bovin coronary and pulmonary arteries. *Am J Physiol Heart Circ Physiol*. 2005; 288: 13–21.
29. **Li JM, Fan LM, George VT, *et al.*** Nox2 regulates endothelial cell cycle arrest and apoptosis *via* p21cip1 and p53. *Free Rad Biol Med*. 2007; 43: 976–86.
30. **Miller AA, Drummond GR, Mast AE, *et al.*** Effect of Gender on NADPH-oxidase activity, expression, and function in the cerebral circulation: role of extrogen. *Stroke*. 2007; 38: 2142–9.
31. **Krijnen PA, Meischl C, Hack CE, *et al.*** Increased Nox2 expression in human cardiomyocytes after acute myocardial infarction. *J Clin Pathol*. 2003; 56: 194–9.
32. **Bennett BL, Sasaky DT, Murray BW, *et al.*** SP600125, an anthrapyrazolone inhibitor of Jun N-terminal kinase. *Proc Natl Acad Sci*. 2001; 98: 13681–6.
33. **L'Ecuyer T, Horenstein MS, Thomas R, *et al.*** Anthracycline-induced cardiac injury using a cardiac cell line: potential for gene therapy studies. *Mol Genet Metab*. 2001; 74: 370–9.
34. **Spallarossa P, Garibaldi S, Altieri P, *et al.*** Carvedilol prevents doxorubicin-induced free radical release and apoptosis in cardiomyocytes *in vitro*. *J Mol Cell Cardiol*. 2004; 37: 837–46.
35. **Turner NA, Xia F, Azhar G, *et al.*** Oxidative stress induces DNA fragmentation and caspase activation *via* the c-Jun NH2-terminal kinase pathway in H9c2 cardiac muscle cells. *J Mol Cell Cardiol*. 1998; 30: 1789–801.
36. **Abas L, Bogoyevitch MA, Guppy M.** Mitochondrial ATP production is necessary for activation of the extracellular-signal regulated kinases during ischaemia/reperfusion in rat myocyte-derived H9c2 cells. *Biochem J*. 2000; 349: 119–26.
37. **Fu J, Lin G, Wu Z, *et al.*** Anti-apoptotic role for C1 inhibitor in ischemia/reperfusion-induced myocardial cell injury. *Biochem Biophys Res Commun*. 2006; 349: 504–12.
38. **Long X, Boluyt MO, Hipolito ML, *et al.*** p53 and the hypoxia-induced apoptosis of cultured neonatal rat cardiac myocytes. *J Clin Invest*. 1997; 99: 2635–43.
39. **Bonavita F, Stefanelli C, Giordano M, *et al.*** H9c2 cardiac myoblasts undergo apoptosis in a model of ischemia consisting of serum deprivation and hypoxia: inhibition by PMA. *FEBS Lett*. 2003; 536: 85–91.
40. **Li JM, Shah AM.** Mechanism of endothelial cell NADPH oxidase activation by angiotensin II. Role of the p47 phox subunit. *J Biol Chem*. 2003; 278: 12094–100.
41. **Meischl C, Krijnen PA, Sipkens JA, *et al.*** Ischemia induces nuclear NOX2 expression in cardiomyocytes and subsequently activates apoptosis. *Apoptosis*. 2006; 11: 913–21.
42. **Frey RS, Rahman A, Kefer JC, *et al.*** PKCs regulates TNF-$\alpha$-induced activation of NADPH oxidase in endothelial cells. *Circ Res*. 2002; 90: 1012–9.
43. **Barnett ME, Madgwick DK, Takemoto DJ.** Protein kinase C as a stress sensor. *Cell Signal*. 2007; 19: 1820–9.
44. **Jung YS, Jung YS, Kim MY, *et al.*** Identification of caspase-independent PKC$\varepsilon$-JNK/p38 MAPK signaling module in response to metabolic inhibition in H9c2 cells. *Jpn J Physiol*. 2004; 54: 23–9.
45. **Rupin A, Paysant J, Sansilvestri-Morel P, *et al.*** Role of NADPH oxidase-mediated superoxide production in the regulation of E-selectin expression by endothelial cells subjected to anoxia/reoxygenation. *Cardiovasc Res*. 2004; 63: 323–30.
46. **Johnson DK, Schillinger KJ, Kwait DM, *et al.*** Inhibition of NADPH oxidase activation in endothelial cells by ortho-methoxy-substituted catechols. *Endothelium*. 2002; 9: 191–203.
47. **Girotti AW.** Lipid hydroperoxide generation, turnover, and effector action in biological systems. *J Lipid Res*. 1998; 39: 1529–42.
48. **McLeod LL, Sevanian A.** Lipid peroxidation and modification of lipid composition in an endothelial cell model of ischemia and reperfusion. *Free Radic Biol Med*. 1997; 23: 680–94.
49. **Martin SF, Chatterjee S, Parinandi N, *et al.*** Rac1 inhibition protects against hypoxia/reoxygenation-induced lipid peroxidation in human vascular endothelial cells. *Vascul Pharmacol*. 2005; 43: 148–56.
50. **Johnson GL, Nakamura K.** The c-jun kinase/stress-activated pathway: regulation, function and role in human disease. *Biochim Biophys Acta*. 2007; 1773: 1341–8.
51. **Steenbergen C.** The role of p38 mitogen-activated protein kinase in myocardial ischemia/reperfusion injury; relationship to ischemic preconditioning. *Basic Res Cardiol*. 2002; 97: 276–85.
52. **Chen JX, Zeng H, Tuo QH, *et al.*** NADPH oxidase modulates myocardial Akt, ERK1/2 activation, and angiogenesis after hypoxia-reoxygenation. *Am J Physiol Heart Circ Physiol*. 2007; 292: H1664–74.
53. **Mizukami Y, Iwamatsu A, Aki T, *et al.*** ERK1/2 regulates intracellular ATP levels through alpha-enolase expression in cardiomyocytes exposed to ischemic hypoxia and reoxygenation. *J Biol Chem*. 2004; 279: 50120–31.
54. **Omura T, Yoshiyama M, Shimada T, *et al.*** Activation of mitogen-activated protein kinases in *in vivo* ischemia/reperfused myocardium in rats. *J Mol Cell Cardiol*. 1999; 31: 1269–79.
55. **Zhao ZQ.** Oxidative stress-elicited myocardial apoptosis during reperfusion. *Curr Opin Pharmacol*. 2004; 4: 159–65.